Published in final edited form as:
Cancer Lett. 2011 July 28; 306(2): 223–229. doi:10.1016/j.canlet.2011.03.010.

Cooperation of the HDAC inhibitor vorinostat and radiation in metastatic neuroblastoma: Efficacy and underlying mechanisms

Sabine Mueller[a,b,e,*], **Xiaodong Yang**[c], **Theo L. Sottero**[c], **Ashley Gragg**[c], **Gautam Prasad**[c], **Mei-Yin Polley**[d], **William A. Weiss**[a,e], **Katherine K. Matthay**[b], **Andrew M. Davidoff**[f], **Steven G. DuBois**[b], and **Daphne A. Haas-Kogan**[c,e]

[a]Department of Neurology, University of California, San Francisco, 505 Parnassus Avenue, San Francisco, CA 94143-0106, USA

[b]Pediatric Hematology/Oncology, University of California, San Francisco, 505 Parnassus Avenue, San Francisco, CA 94143-0106, USA

[c]Department of Radiation Oncology, University of California, San Francisco, Helen-Diller Family Cancer Research Center, 1450 3rd Street, San Francisco, CA 94158, USA

[d]National Cancer Institute, Biometric Research Branch, Executive Plaza North, Room 8124, 6130 Executive Boulevard, Rockville, MD 20852, USA

[e]Department of Neurosurgery, University of California, San Francisco, 400 Parnassus Avenue, San Francisco, CA 94117, USA

[f]Department of Surgery, St. Jude Children's Research Hospital, 262 Danny Thomas Place, Memphis, TN 38105-3678, USA

Abstract

Histone deacetylase (HDAC) inhibitors can radiosensitize cancer cells. Radiation is critical in high-risk neuroblastoma treatment, and combinations of HDAC inhibitor vorinostat and radiation are proposed for neuroblastoma trials. Therefore, we investigated radiosensitizing effects of vorinostat in neuroblastoma. Treatment of neuroblastoma cell lines decreased cell viability and resulted in additive effects with radiation. In a murine metastatic neuroblastoma *in vivo* model vorinostat and radiation combinations decreased tumor volumes compared to single modality. DNA repair enzyme Ku-86 was reduced in several neuroblastoma cells treated with vorinostat. Thus, vorinostat potentiates anti-neoplastic effects of radiation in neuroblastoma possibly due to down-regulation of DNA repair enzyme Ku-86.

Keywords

Metastatic neuroblastoma; Radiation; Vorinostat; DNA repair

[*]Corresponding author at: Department of Neurology, University of California, San Francisco, 505 Parnassus Avenue, M688, Box 0106, San Francisco, CA 94143-0106, USA. Tel.: +1 415 476 3831; fax: +1 415 502 4372. muellers@neuropeds.ucsf.edu (S. Mueller).

Conflict of interest

None of the authors have any conflicts of interest to report.

1. Introduction

Neuroblastoma is the most common extra-cranial tumor of childhood with approximately 650 new cases per year in the United States. The clinical presentation is heterogeneous and dependent on age at diagnosis, staging, histology, and genetic alterations such as *MYCN* amplification and losses of chromosome 1p and 11q. High-risk patients with evidence of metastases have an overall survival (OS) rate of less than 40% despite intensive multi-modality treatment, highlighting the urgent need for new treatment strategies.

External beam radiation plays key roles in the treatment of primary tumor and metastatic sites in patients with high-risk neuroblastoma. In addition, targeted radiotherapy with ^{131}I-metaiodobenzylguanidine (MIBG) is a promising treatment approach with 30% response rates in refractory disease [1]. MIBG, a norepinephrine analog, is taken up by the norepinephrine transporter (NET) that is abundantly expressed on neuroblastoma cells. Newer treatment strategies are focusing on combining ^{131}I-MIBG with radiosensitizing agents.

Histone deacetylase (HDAC) inhibition using small molecules is an emerging concept to alter gene expression in the treatment of cancer. Vorinostat (also known as suberoylanilide hydroxamic acid, SAHA) is a pan HDAC inhibitor that is the first agent in its class to be approved by the Food and Drug Administration (FDA) for the treatment of cutaneous T-cell lymphoma. Several studies have shown that HDAC inhibitors have radiosensitizing effects in a variety of cancer models [2–7] and vorinostat in particular demonstrates promising results as a radiation sensitizer in phase I clinical trials [8]. The underlying mechanisms for the radiosensitizing effects of HDAC inhibitors are not fully understood. Vorinostat inhibits expression of double-strand break repair enzymes such as Rad51 and Ku-86 and prolongs expression of phosphorylated H2AX (γ-H2AX) [3,9]. These findings suggest that vorinostat sensitizes cells to radiation by inhibiting repair of radiation-induced DNA damage [2,7].

Several clinical trials are testing vorinostat in combination with chemotherapy and/or radiation in a variety of adult cancers, including brain and pancreatic tumors. The Children's Oncology Group (COG) is currently testing the safety and efficacy of vorinostat with isotretinoin for the treatment of solid tumors, lymphoma, and leukemia as well as in combination with radiation for malignant gliomas in children. The favorable toxicity profiles reported in these ongoing trials render HDAC inhibitors promising agents for cancer therapy in children. This study establishes the pre-clinical rationale for clinical studies for the treatment of high-risk neuroblastoma with the combination of vorinostat and either external beam radiotherapy or targeted radiation in the form of ^{131}I-MIBG.

2. Materials and methods

2.1. Cell lines and treatments

NB1691 cells expressing the luciferase gene (NB1691^{luc}) [10] were cultured in RPMI-1640 with 10% heat-inactivated fetal bovine serum, 100 U/ml penicillin (GIBCO BRL, Gaithersburg MD), and 100 μg/ml streptomycin (GIBCO BRL, Gaithersburg, MD). Intermittently, NB1691^{luc} cells were treated with 100 μg/ml Zeocin (InvivoGen, San Diego, CA) for selection of the luciferase gene. The neuroblastoma cell lines Kelly, SY5Y and *MYCN* inducible Tet21 [11], were grown in DMEM (GIBCO BRL, Gaithersburg MD) with 10% heat-inactivated fetal bovine serum (GIBCO BRL, Gaithersburg MD), 100 U/ml penicillin (GIBCO BRL, Gaithersburg MD), and 100 μg/ml streptomycin (GIBCO BRL, Gaithersburg, MD). Doxycycline, 1 μg/μl, was added to the Tet21 cells to suppress *MYCN* expression. Cultures were maintained at 37 °C and 8% CO_2. Vorinostat (supplied by Merck, NJ, USA) was reconstituted in DMSO at 10 mg/ml, stored at −20 °C, and appropriate fresh

dilutions made immediately prior to each experiment. Concentrations of DMSO in *in vitro* experiments were kept less than 0.1%. Control cells were treated with the same amount of DMSO to control for possible cytotoxic effects of DMSO alone. Cultures were irradiated using a cesium source at a dose rate of 1.97 Gy/min using the specified total doses.

2.2. Clonogenic survival assay

For clonogenic assays, single-cell suspensions were generated for each cell line and specified numbers of cells were seeded into six-well tissue culture plates. Cells were allowed to adhere for 16 h, treated with 0.5 μM vorinostat (a concentration that resulted in reduction in viability of 0.5–1 log), and then irradiated 3 h later. Two to three weeks after seeding, depending on each individual cell line, colonies were stained with crystal violet. For the NB1691 and Tet21 (with doxycycline) colonies were stained after 3 weeks; for SY5Y, Kelly and Tet21 (without doxycycline) colonies were stained after 2 weeks. Colonies of greater than 50 cells were counted to determine the surviving fraction. Surviving fractions were normalized to the plating efficiency of each cell line [12]. The data presented are the mean ± standard error (SE) and represent four independent experiments.

2.3. Metastatic neuroblastoma model and treatment

Athymic *Foxn1*^{nu} mice (Taconic, Hudson NY), 4–6 weeks of age, were used for all *in vivo* experiments. All procedures were performed according to a protocol approved by University of California, San Francisco (UCSF) Institutional Animal Care and Use Committee. A model of metastatic neuroblastoma was established by tail vein injecting of 6×10^6 NB1691^{luc} cells. This model is slightly modified from prior publication [10]. In our model we used athymic mice and injected 6×10^6 NB1691^{luc} cells whereas Dickson et al. used SCID mice and injected 2×10^6 NB1691^{luc} cells. Representative tumors were collected and fixed in 10% buffered formalin, embedded in paraffin, sectioned at 250 μm intervals, and stained with hematoxillin–eosin (H&E). Mice were treated with vorinostat 150 mg/kg intraperitoneal (IP), radiation, or combinations thereof. Treatment started 7 days after tail vein injection of NB1691^{luc} cells. Mice received a total of three treatments that were administered on days 7, 9 and 11 after tumor inoculation. Each treatment group contained 10 mice. Since in all tumor-bearing mice metastatic neuroblastoma was detected in all parts of the body except the head, 1 Gy of radiation was administered to the entire animal's body while shielding the head and pharynx. Radiation was performed 1 h after IP administration of either vorinostat or DMSO as a control. All animals were anesthetized with ketamine/xylazine prior to irradiation.

2.4. Bioluminescence imaging

In vivo bioluminescence images were obtained using the IVIS Imaging System 100 series (Xenogen Cooperation, Alameda, CA). Mice were injected with 150 mg/kg IP D-luciferin. Thirteen minutes after injection, mice anesthetized with isoflurane were imaged using various exposure times (ranging from 2 s to 5 min) to optimize images. Whole body bioluminescence was measured for each mouse. The mean bioluminescence for each treatment group was calculated and *p*-values of group comparisons were based on Wilcoxon rank-sum test. The last measurement used in the analysis was the last day all mice were alive.

2.5. Western blot analyses

Effects of vorinostat on acetylation of histone 4 (H4) in tumor samples were determined by western blot analysis. The metastatic model of NB1691^{luc} in athymic mice was established as described above. As soon as tumor was detectable via bioluminescence, mice were treated with 150 mg/kg of vorinostat and/or radiation. Radiation was performed 1 h after IP

injection of vorinostat. Mice were sacrificed according to guidelines of the Animal Care and Use Committee at UCSF at specified times points (1, 3, 6, and 24 h after vorinostat administration). Tumors were snap frozen in liquid nitrogen and homogenized. Histones were purified as described previously [5]. Briefly, histones were purified with H_2SO_4 (0.2 mol/L) for 1 h and then dialyzed once against 0.1 mol/L acetic acid for 2 h and twice against water for 2 h. A fourth dialysis was performed overnight against water with 50% glycerol. Whole protein lysates from tumors were obtained by using lysis buffer (50 mM Tris.HCl, 150 mM NaCl,1 mM EDTA, 1% Triton X-100, 0.1% SDS) and a proteinase inhibitor cocktail tablet (Roche Diagnostics Corporation, Indianapolis, IN).

For *in vitro* samples, cells were lysed with RIPA buffer and incubated with proteinase inhibitor cocktail (Roche Diagnostics Corporation, Indianapolis, IN). Thirty micrograms of protein lysate were separated by gel electrophoresis using 4–20% of Tris–Glycine gels (Invitrogen, Carlsbad, CA) and transferred to PVDF membranes. Membranes were blocked with 4% nonfat dry milk in 0.1% Tween 20 Tris-buffered saline for 1 h at room temperature. Subsequently membranes were incubated with primary antibody overnight at 4 ° C. Blots were washed with 0.1% Tween 20 Tris-buffered saline for 15 min × 3 and then incubated for 1 h at room temperature with secondary antibody. Bands were visualized using ECL-chemiluminescence substrate (Amersham Pharmacia, Buckinghamshire, UK) and quantified using Image J (National Institute of Health). Antibodies against acetylated H4, total H3, Rad51, XRCC4-Like-Factor (XLF), and Ku86 were obtained from Cell Signaling Technology (Danvers, MA), anti-β-actin antibody from Sigma–Aldrich (St. Louis, MO), and anti-rabbit and anti-mouse antibodies from Amersham Pharmacia (Buckinghamshire, UK).

2.6. Detection of γ-H2AX by flow cytometry

$NB1691^{luc}$ cells were treated with 0.5, 1, or 2.5 μM of vorinostat for 24 h followed by 2 Gy of ionizing radiation. Cells were harvested 6 h after radiation exposure. Phosphorylated H2AX (γ-H2AX) was detected using a flow cytometry H2AX kit (Upstate, NY). Cells were harvested by trypsin–EDTA, washed with PBS three times and fixed according to manufacturer's guidelines (Upstate, NY). Cells were washed and resuspended in permeabilization solution to a final concentration of 2×10^6 cells/ml. The anti-phospho-histone H2AX, fluorescein isothiocyanate (FITC) conjugate was added to the cells and incubated for 20 min on ice. As a negative control cells were incubated with IgG–FITC conjugate. Cells were washed and suspended in FACS buffer. Samples were analyzed using a BD Biosciences FACS Calibur cytometer (San Jose, CA). The data presented are the mean ± standard error (SE) and represent two independent experiments.

3. Results

3.1. Radiosensitization of neuroblastoma cells in vitro by vorinostat

Clonogenic survival assays are the gold standard for radiosensitization experiments and therefore such assays were carried out in four different neuroblastoma cell lines. Neuroblastoma cells lines $NB1691^{luc}$ (*MYCN* amplified), Kelly (*MYCN* amplified), SY5Y (*MYCN* non-amplified) and *MYCN* inducible Tet21 were treated with 0.5 μM of vorinostat. We chose vorinostat doses that in single agent experiments (see Supplementary Fig. S1) resulted in reduction in viability of 0.5–1 log in the investigated cell lines. Fig. 1 demonstrates additive cytotoxicity produced by combination of vorinostat and radiation. Table 1 shows cell surviving fractions following specified radiation doses with and without vorinostat.

3.2. Radiosensitization by vorinostat in vivo in a metastatic neuroblastoma model

To establish the effects of vorinostat and radiation *in vivo*, a meta-static neuroblastoma model was established by tail vein injection of NB1691^{luc} cells in athymic mice [10,13]. Mice developed widely meta-static tumor that was visible by bioluminescence 21 days after tumor injection in 100% of animals. Fig. 2A shows an example of five mice bearing metastatic neuroblastoma. Histological examination confirmed that areas of bioluminescence signal corresponded to neuroblastoma formation as shown in Fig. 2B.

To evaluate effects of vorinostat, radiation, and combinations thereof, we first assessed toxicity of various regimens. Initial experiments with daily administration of vorinostat IP at doses of 50–150 mg/kg (average treatment length of 20 days) were associated with excessive toxicities manifested by weight loss, particularly in the combination groups. We therefore opted to administer vorinostat less frequently but at higher doses per injection, a regimen that proved both well-tolerated and efficacious. Mice were treated with vorinostat 150 mg/kg IP every other day, three doses total; in the combination group 1 Gy of radiation followed each dose of vorinostat 1 h later for a total of 3 Gy. Analyses comparing tumor volumes among different treatment groups were performed at the last time point all animals were still alive. As shown in Fig. 3, combination of vorinostat and radiation had striking anti-tumor activity, resulting in tumor volumes that were significantly smaller compared to either vorinostat or radiation alone ($p = 0.04$ for each comparison).

To document biochemical consequences of vorinostat and radiation therapy *in vivo* in metastatic neuroblastoma, we quantified histone acetylation in tumor-bearing mice following various treatment regimens. Histones were purified at specified times following vorinostat administration (1, 3, 6, and 24 h after vorinostat) and acetylation of H4 was analyzed by western blot analysis. Combination of vorinostat and radiation increased levels of acetylated H4, 1 h after treatment and remained elevated compared to control for 24 h (data not shown).

3.3. Effects of vorinostat and radiation on γ-H2AX expression in NB1691^{luc} cells

Multiple studies have shown that in several different cancer types vorinostat prolongs the appearance of serine 139-phosphorylated histone H2AX (γ-H2AX). Since many early components of DNA repair pathways co-localize with γ-H2AX at sites of DNA double-strand breaks (DSBs), quantification of γ-H2AX reflects induction of DSBs and furthermore, prolongation of γ-H2AX expression suggests that DNA repair mechanisms are impaired after HDAC inhibitor exposure [2,7]. To explore effects of radiation and vorinostat on DNA repair mechanisms we quantified γ-H2AX appearance in NB1691^{luc} cells by flow cytometry after treatment. NB1691^{luc} cells were treated with vorinostat (0.5, 1 or 2.5 μm), irradiated 24 h later with 2 Gy, and harvested 6 h after irradiation. Fig. 4 demonstrates that increasing concentrations of vorinostat resulted in dose-dependent elevations in γ-H2AX expression levels in NB1691^{luc} cells compared to control-treated cells (control: 2.5%; 0.5 μm: 9.8%; 1 μm: 20.3%; and 2.5 μm: 21.3% γ-H2AX expression). Cells treated with a combination of radiation and vorinostat showed not only a dose-dependent elevation of γ-H2AX but also higher expression levels than either treatment modality alone (2 Gy: 6%; 0.5 μm + 2 Gy: 19.7%; 1 μM + 2 Gy: 31.6%; and 2.5 μm + 2 Gy: 37%).

3.4. Effect of vorinostat and radiation on DNA repair enzymes

Enhanced and sustained expression of γ-H2AX following combined treatment with radiation and vorinostat suggest that vorinostat impairs repair of DNA DSBs. We sought to test the hypothesis that vorinostat blunts DSB repair by reducing expression of DNA repair genes. DNA DSBs are repaired by either homologous recombination (HR) or non-homologous end-joining (NHEJ). Rad51 plays an important role in HR [14]. Decreased Rad51 expression is

associated with increased radiosensitivity [9] and one study found that treatment of prostate cancer cells with vorinostat attenuated expression of Rad51 [3]. We assessed expression of Rad51 in NB1691^{luc} cells following treatment and found that Rad51 expression did not change significantly after vorinostat or radiation exposure at two different time points. In contrast to Rad51, expression of another DNA repair protein, Ku-86, was decreased by vorinostat treatment (Fig. 5). Ku-86, key to the NHEJ pathway, has been shown to be down-regulated in melanoma cells after treatment with HDAC inhibitor [15]. In our model system of neuroblastoma expression of Ku-86 was similarly decreased after vorinostat treatment in a dose-dependent manner (0.5 μM and 2.5 μM) in two independent cell lines NB1691^{luc} and SY5Y (see Supplementary Fig. S2), an effect that was not abolished by irradiation and was sustained for up to 24 h after vorinostat treatment. Recently XLF (XRCC4 Like Factor), also called Cernunnos, was identified as an additional participant in the NHEJ pathway [16]. The expression of XLF however, was not affected by the treatment of vorinostat, radiation or a combination thereof as shown in Fig. 5.

4. Discussion

Several clinical trials are investigating vorinostat in combination with chemotherapy or radiation in the management of adult malignancies. Recently a phase I study combining vorinostat with ^{131}I-MIBG for recurrent neuroblastoma was initiated. The favorable toxicity profile and radiosensitizing effects render vorinostat an ideal candidate to combine with radiation for childhood cancers. Radiation plays a key role in the treatment of high-risk neuroblastoma, using external beam radiation or targeted radioisotopes such as ^{131}I-MIBG [17]. With the goal of establishing the pre-clinical rationale for combining vorinostat and radiation for neuroblastoma, we investigated the radiosensitizing effects of this HDAC inhibitor in neuroblastoma cells *in vitro* as well as in a human xenograft mouse model of metastatic neuroblastoma. *In vitro*, we demonstrated that neuroblastoma cells were sensitive to vorinostat treatment and showed an additive effect with radiation therapy in neuroblastoma cell lines. We did not observe a correlation between the MYCN status and response to vorinostat. The additive effect of radiation and vorinostat was present even at lower vorinostat concentrations (0.5 μM). This is of clinical importance since serum concentrations in humans rarely exceed 2 μM after oral administration [18].

For our *in vivo* experiments, we used the NB1691 neuroblastoma cell line, modified with the luciferase gene that enables *in vivo* monitoring of tumor burden without sacrificing the animals [10]. In these *in vivo* experiments combination of vorinostat and radiation exhibited dramatic anti-tumor activity, significantly superior to either modality alone. Prior studies using colorectal carcinoma, melanoma, glioma, and prostate cancer demonstrated similar radiosensitizing effects of HDAC inhibitors [2,3,5,6]. In our model, increased histone acetylation persisted *in vivo* for at least 24 h after drug administration. In other studies increased histone acetylation was also present shortly after vorinostat administration (3 h) but returned to baseline within 12 h. Such issues of sequencing and timing of vorinostat and radiation have bearing on ongoing and planned clinical trials. As the New Approaches to Neuroblastoma Therapy (NANT) Consortium was planning its recently opened study of vorinostat and ^{131}I-MIBG for resistant/relapsed neuroblastoma, decisions regarding the timing of drug and ^{131}I-MIBG administration were informed by the results described herein. Since elevated histone acetylation was documented within 1 h of vorinostat administration *in vivo* and was sustained for at least 24 h, children on NANT N2007-03 receive vorinostat on days 1 and 2 prior to ^{131}I-MIBG therapy, on day 3, 1 h before ^{131}I-MIBG administration, and for a 10 day course thereafter. Furthermore, correlative biology studies include evaluation of peripheral blood mononuclear cell (PBMC) histone acetylation and whole blood norepinephrine transporter mRNA levels on day 1 prior to the first dose of vorinostat, on day 3 prior to the third dose of vorinostat, on day 3, 1 h after vorinostat, just prior to ^{131}I-

MIBG infusion, and on day 12, 13, or 14, 1 h after vorinostat. These histone acetylation levels and their changes relative to baseline will be used to explore possible associations with toxicities and with tumor responses or prolonged progression-free intervals. However, it should be noted that some investigators also shown that the presence of hyperacetylation is not required for the radiosensitizing effect of vorinostat [6].

The underlying mechanisms of HDAC inhibitor-mediated radiosensitization are not fully understood but effects on DNA repair enzyme expression levels have been previously implicated [2,3,19]. Several investigations have shown increased expression of γ-H2AX after vorinostat exposure suggesting impairment of DNA repair [2,7]. Our current study demonstrates that combination of radiation and vorinostat increased γ-H2AX expression significantly more than either treatment modality alone, corroborating prior indications that HDAC inhibitor-mediated radiosensitization is due to inhibitory effects on DNA repair enzymes. Indeed, expression of Ku-86, a key component of NHJE, was reduced in a dose-dependent manner after treatment with vorinostat in two independent neuroblastoma cell lines. However, whereas others have reported that vorinostat reduces expression of both Rad51 and Ku-86 [3,15,20], we found no change in Rad51 expression following vorinostat treatment. This discrepancy may be due to higher vorinostat concentrations used in these studies while we chose to use lower, more physiologic vorinostat doses [15,20]. To further assess the NHJE pathway we assessed the expression of another NHJE factor, XLF. We did not observe reduced expression of this factor after vorinostat treatment, suggesting that vorinostat radiosensitizes neuroblastoma cells by impairing Ku-86 but not XLF. Moreover, others have shown that histone deacetylases are implicated as essential components of the DNA repair process itself and the comprehensive mechanism of HDAC inhibitor radiosensitization remains to be elucidated [21].

The role of radiation is well established in the treatment of metastatic neuroblastoma and promising results have stimulated interest in introducing HDAC inhibitors into multi-modality therapy for this common pediatric solid tumor. Several studies under consideration propose to combine vorinostat with radiation. Our study provides a strong pre-clinical rationale of combining radiation with vorinostat in neuroblastoma. However we did not assess the effect of targeted radiation such as ^{131}I-MIBG in our study. Interactions of targeted radiation therapy with vorinostat may differ from conventional radiation therapy. A recently activated phase 1 clinical study is testing vorinostat in combination with ^{131}I-MIBG for high-risk neuroblastoma.

Supplementary Material

Refer to Web version on PubMed Central for supplementary material.

Acknowledgments

Funding

This research was supported in part by NIH-PO1 NS-42927-27A2 (DHK), PO1 CA81403 (KKM), NIH Brain Tumor SPORE Grant P50 CA097257 (DHK, MYP, WAW), NIH/NCRR/OD UCSF-CTSI Grant No. KL2 RR024130 (SGD), NIH-R01CA133091 (WAW), The Nancy and Stephen Grand Philanthropic Fund (DAH-K), The V Foundation (DHK, KKM, WAW), Dougherty Foundation (KKM), Thrasher Foundation (WAW, KKM, DHK), Alex's Lemonade Stand Foundation (KKM), Campini Foundation (SM, KKM, SGD).

References

1. Matthay KK, Yanik G, Messina J, Quach A, Huberty J, Cheng SC, Veatch J, Goldsby R, Brophy P, Kersun LS, Hawkins RA, Maris JM. Phase II study on the effect of disease sites, age, and prior

therapy on response to iodine-131-metaiodobenzylguanidine therapy in refractory neuroblastoma. J Clin Oncol. 2007; 25:1054–1060. [PubMed: 17369569]

2. Munshi A, Tanaka T, Hobbs ML, Tucker SL, Richon VM, Meyn RE. Vorinostat, a histone deacetylase inhibitor, enhances the response of human tumor cells to ionizing radiation through prolongation of gamma-H2AX foci. Mol Cancer Ther. 2006; 5:1967–1974. [PubMed: 16928817]
3. Chinnaiyan P, Vallabhaneni G, Armstrong E, Huang SM, Harari PM. Modulation of radiation response by histone deacetylase inhibition. Int J Radiat Oncol Biol Phys. 2005; 62:223–229. [PubMed: 15850925]
4. Entin-Meer M, Rephaeli A, Yang X, Nudelman A, VandenBerg SR, Haas-Kogan DA. Butyric acid prodrugs are histone deacetylase inhibitors that show antineoplastic activity and radiosensitizing capacity in the treatment of malignant gliomas. Mol Cancer Ther. 2005; 4:1952–1961. [PubMed: 16373710]
5. Entin-Meer M, Yang X, VandenBerg SR, Lamborn KR, Nudelman A, Rephaeli A, Haas-Kogan DA. In vivo efficacy of a novel histone deacetylase inhibitor in combination with radiation for the treatment of gliomas. Neuro Oncol. 2007; 9:82–88. [PubMed: 17347490]
6. Folkvord S, Ree AH, Furre T, Halvorsen T, Flatmark K. Radiosensitization by SAHA in experimental colorectal carcinoma models-in vivo effects and relevance of histone acetylation status. Int J Radiat Oncol Biol Phys. 2009; 74:546–552. [PubMed: 19427556]
7. Baschnagel A, Russo A, Burgan WE, Carter D, Beam K, Palmieri D, Steeg PS, Tofilon P, Camphausen K. Vorinostat enhances the radiosensitivity of a breast cancer brain metastatic cell line grown in vitro and as intracranial xenografts. Mol Cancer Ther. 2009; 8:1589–1595. [PubMed: 19509253]
8. Ree AH, Dueland S, Folkvord S, Hole KH, Seierstad T, Johansen M, Abrahamsen TW, Flatmark K. Vorinostat, a histone deacetylase inhibitor, combined with pelvic palliative radiotherapy for gastrointestinal carcinoma: the Pelvic Radiation and Vorinostat (PRAVO) phase 1 study. Lancet Oncol. 11:459–464. [PubMed: 20378407]
9. Taki T, Ohnishi T, Yamamoto A, Hiraga S, Arita N, Izumoto S, Hayakawa T, Morita T. Antisense inhibition of the RAD51 enhances radiosensitivity. Biochem Biophys Res Commun. 1996; 223:434–438. [PubMed: 8670299]
10. Dickson PV, Hamner B, Ng CY, Hall MM, Zhou J, Hargrove PW, McCarville MB, Davidoff AM. In vivo bioluminescence imaging for early detection and monitoring of disease progression in a murine model of neuroblastoma. J Pediatr Surg. 2007; 42:1172–1179. [PubMed: 17618876]
11. Lutz W, Stohr M, Schurmann J, Wenzel A, Lohr A, Schwab M. Conditional expression of N-myc in human neuroblastoma cells increases expression of alpha-prothymosin and ornithine decarboxylase and accelerates progression into S-phase early after mitogenic stimulation of quiescent cells. Oncogene. 1996; 13:803–812. [PubMed: 8761302]
12. Franken NA, Rodermond HM, Stap J, Haveman J, van Bree C. Clonogenic assay of cells in vitro. Nat Protoc. 2006; 1:2315–2319. [PubMed: 17406473]
13. Rosati SF, Williams RF, Nunnally LC, McGee MC, Sims TL, Tracey L, Zhou J, Fan M, Ng CY, Nathwani AC, Stewart CF, Pfeffer LM, Davidoff AM. IFN-beta sensitizes neuroblastoma to the antitumor activity of temozolomide by modulating O6-methylguanine DNA methyltransferase expression. Mol Cancer Ther. 2008; 7:3852–3858. [PubMed: 19056675]
14. Jackson SP. Sensing and repairing DNA double-strand breaks. Carcinogenesis. 2002; 23:687–696. [PubMed: 12016139]
15. Munshi A, Kurland JF, Nishikawa T, Tanaka T, Hobbs ML, Tucker SL, Ismail S, Stevens C, Meyn RE. Histone deacetylase inhibitors radiosensitize human melanoma cells by suppressing DNA repair activity. Clin Cancer Res. 2005; 11:4912–4922. [PubMed: 16000590]
16. Ahnesorg P, Smith P, Jackson SP. XLF interacts with the XRCC4-DNA ligase IV complex to promote DNA nonhomologous end-joining. Cell. 2006; 124:301–313. [PubMed: 16439205]
17. DuBois SG, Matthay KK. Radiolabeled metaiodobenzylguanidine for the treatment of neuroblastoma. Nucl Med Biol. 2008; 35(Suppl 1):S35–S48. [PubMed: 18707633]
18. Ramalingam SS, Parise RA, Ramanathan RK, Lagattuta TF, Musguire LA, Stoller RG, Potter DM, Argiris AE, Zwiebel JA, Egorin MJ, Belani CP. Phase I and pharmacokinetic study of vorinostat, a

histone deacetylase inhibitor, in combination with carboplatin and paclitaxel for advanced solid malignancies. Clin Cancer Res. 2007; 13:3605–3610. [PubMed: 17510206]

19. Adimoolam S, Sirisawad M, Chen J, Thiemann P, Ford JM, Buggy JJ. HDAC inhibitor PCI-24781 decreases RAD51 expression and inhibits homologous recombination. Proc Natl Acad Sci USA. 2007; 104:19482–19487. [PubMed: 18042714]
20. Lee JH, Choy ML, Ngo L, Foster SS, Marks PA. Histone deacetylase inhibitor induces DNA damage, which normal but not transformed cells can repair. Proc Natl Acad Sci USA. 107:14639–14644.
21. Masumoto H, Hawke D, Kobayashi R, Verreault A. A role for cell-cycle-regulated histone H3 lysine 56 acetylation in the DNA damage response. Nature. 2005; 436:294–298. [PubMed: 16015338]

Appendix A. Supplementary material

Supplementary data associated with this article can be found, in the online version, at doi: 10.1016/j.canlet.2011.03.010.

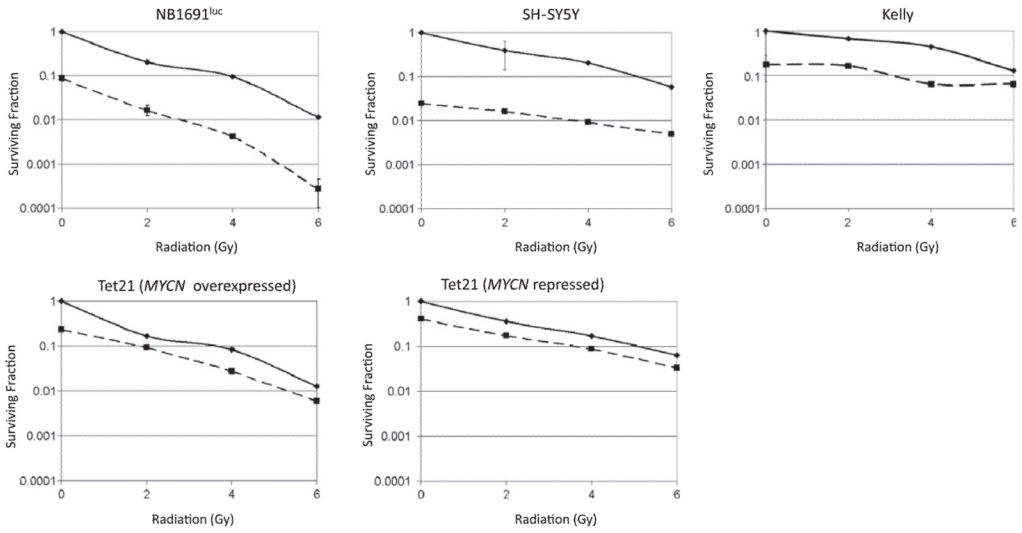

Fig. 1.

Clonogenic survival assays of neuroblastoma cell lines NB1691^{luc}, SY5Y, Kelly, Tet21 (*MYCN* overexpressed), and Tet21 (*MYCN* repressed) treated with vorinostat and radiation. Surviving fractions are normalized to control samples for each treatment group. Solid line: radiation alone; dashed line: 0.5 μM vorinostat pre-treatment followed by radiation. All experiments were performed in quadruplicate. Surviving fractions are shown on a log scale as mean and bars represent standard error of the mean; where errors are not visualized, the error bars are smaller than the size of the symbol.

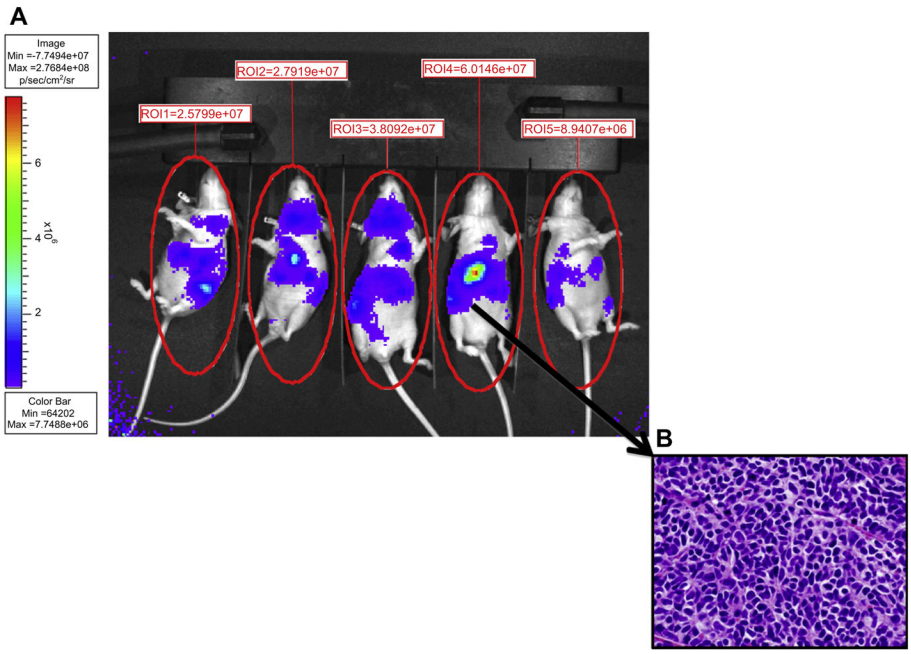

Fig. 2.

(A) *In vivo* model of metastatic neuroblastoma in athymic mice. Mice were injected by tail vein with 6×10^6 $NB1691^{luc}$ cells. Approximately 21 days after injection all mice demonstrated visible tumors by bioluminescence. Tumor volumes for each mouse were quantified by measuring the whole mouse body emission of photons in a standardized fashion. (B) Immunohistological hematoxillin–eosin (H&E) stain of a representative tumor.

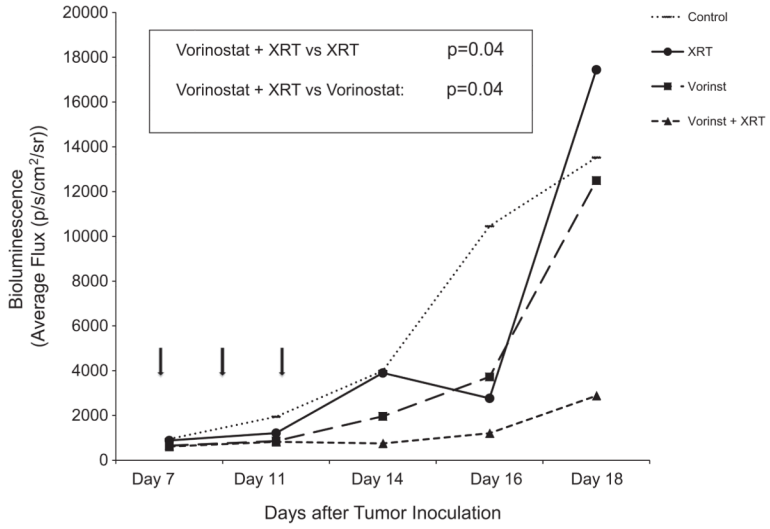

Fig. 3.

In vivo efficacy of combined vorinostat (vorinst) and radiation in the treatment of metastatic neuroblastoma. Seven days after tail vein injection of NB1691^{luc} cells, mice were treated with intraperitoneal vorinostat (150 mg/kg) every other day for a total of three doses, radiation (1 Gy) every other day for a total of 3 Gy, or combination of vorinostat (150 mg/kg) followed by radiation (1 Gy delivered 1 h after vorinostat). Each treatment group contained 10 mice. Arrows indicate treatment days. Bioluminescence imaging was performed until the first mouse died. *p*-Values of group comparisons are based on Wilcoxon Rank-Sum test and were calculated as vorinostat versus combination of vorinostat and radiation ($p = 0.04$) and radiation versus combination of vorinostat and radiation ($p = 0.04$). Control group is represented by dotted line, radiation (XRT) alone by solid line, vorinostat (vorinst) alone by small dashed, and combination group by large dashed line.

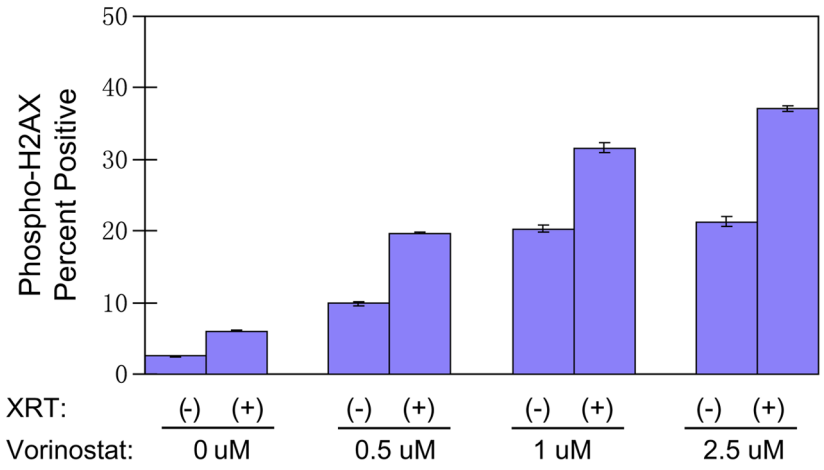

Fig. 4.

γ-H2AX expression levels after vorinostat and radiation (XRT) treatment measured by flow cytometric analysis of NB1691^{luc} cells. Cells were incubated with vorinostat at (0.5 μM, 1 μM, or 2.5 μM) for 24 h and irradiated with 2 Gy 24 h later. Cells were harvested 6 h after radiation. Percent of cells positive for γ-H2AX staining is shown on the *y*-axis.

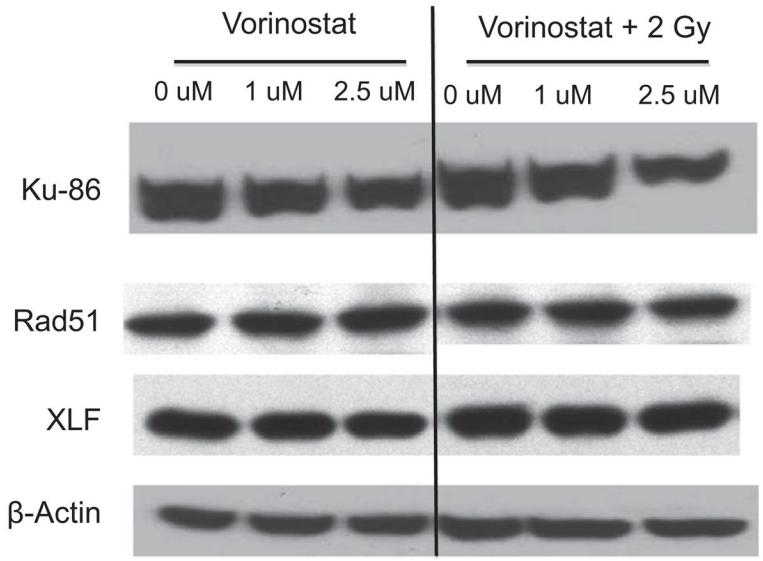

Fig. 5.

Western blot analysis of Ku-86, XRCC4 Like Factor (XLF), and Rad51 expression in NB1691^{luc} cells after vorinostat and radiation treatment. Cells were treated with vorinostat (1.0 μM or 2.5 μM), 2 Gy of radiation, or combination treatment. Cells were harvested 24 h after radiation. β-Actin was used as a loading control.

Table 1

Surviving fractions following treatment with vorinostat and radiation in clonogenic assays.

Radiation dose (Gy)	Vorinostat									
	NB1691^{luc} (*MYCN* amplified)		Tet21 (*MYCN* repressed)		Tet21 (*MYCN* overexpressed)		SY5Y (*MYCN* non-amplified)		Kelly (*MYCN* amplified)	
	(−)	(+)	(−)	(+)	(−)	(+)	(−)	(+)	(−)	(+)
0	1.12×10^{-1}	9.72×10^{-3}	6.50×10^{-2}	1.31×10^{-2}	8.50×10^{-2}	1.44×10^{-2}	5.52×10^{-2}	1.36×10^{-3}	1.12×10^{-2}	2.00×10^{-3}
2	2.28×10^{-2}	1.85×10^{-3}	1.21×10^{-2}	3.13×10^{-3}	1.29×10^{-2}	1.88×10^{-3}	2.20×10^{-2}	8.96×10^{-4}	7.60×10^{-3}	1.86×10^{-3}
4	1.05×10^{-2}	4.63×10^{-4}	4.27×10^{-3}	1.09×10^{-3}	2.50×10^{-3}	9.38×10^{-4}	1.12×10^{-3}	5.12×10^{-4}	4.96×10^{-3}	7.20×10^{-4}
6	1.27×10^{-3}	6.17×10^{-5}	7.03×10^{-4}	3.13×10^{-4}	1.09×10^{-3}	1.56×10^{-4}	3.20×10^{-4}	2.72×10^{-4}	1.44×10^{-3}	7.20×10^{-4}